

Plantain and Banana Starches: Granule Structural Characteristics Explain the Differences in Their Starch Degradation Patterns

Claudinéia Aparecida Soares,[†] Fernanda Helena Gonçalves Peroni-Okita,[†] Mateus Borba Cardoso,[‡] Renata Shitakubo,[†] Franco Maria Lajolo,[†] and Beatriz Rosana Cordenunsi^{*,†}

[†]Laboratório de Química, Bioquímica e Biologia Molecular de Alimentos, Departamento de Alimentos e Nutrição Experimental, FCF, Universidade de São Paulo, Avenida Lineu Prestes 580, Bloco 14, CEP 05508-900, São Paulo (SP), Brazil

[‡]Laboratório Nacional de Luz Síncrotron (LNLS), Caixa Postal 6192, CEP 13083-970, Campinas, SP, Brazil

 Supporting Information

ABSTRACT: Different banana cultivars were used to investigate the influences of starch granule structure and hydrolases on degradation. The highest degrees of starch degradation were observed in dessert bananas during ripening. Scanning electron microscopy images revealed smooth granule surface in the green stage in all cultivars, except for Mysore. The small and round granules were preferentially degraded in all of the cultivars. Terra demonstrated a higher degree of crystallinity and a short amylopectin chain length distribution, resulting in high starch content in the ripe stage. Amylose content and the crystallinity index were more strongly correlated than the distribution of amylopectin branch chain lengths in banana starches. α - and β -amylase activities were found in both forms, soluble in the pulp and associated with the starch granule. Starch-phosphorylase was not found in Mysore. On the basis of the profile of α -amylase in vitro digestion and the structural characteristics, it could be concluded that the starch of plantains has an arrangement of granules more resistant to enzymes than the starch of dessert bananas.

KEYWORDS: Banana, starch granule, structure, amylose, amylopectin, crystallinity, α -amylase, β -amylase, starch-phosphorylases, in vitro digestion

INTRODUCTION

Banana (cv. Nanicão) accumulates a large amount of starch (~20%) during fruit development, which is converted into soluble sugars (mainly sucrose) during ripening.^{1,2} This metabolism is an efficient, coordinated, and complex enzymatic process, which converts starch into soluble sugars in a relatively short time scale (~4 days).^{1,3,4}

Our group has demonstrated that the enzymes involved in starch degradation, such as α -amylase, β -amylase, isoamylases, starch-phosphorylases, and sucrose phosphate synthase, are present in banana pulp (cv. Nanicão).^{5–8} However, the exact contribution of each enzyme in this process remains unknown.

On the basis of their genomic composition, edible bananas can be classified as diploid (AA and AB), triploid (AAA, AAB, and ABB), or tetraploid (AAAA, AAAB, and AABB). However, the most relevant bananas are mainly triploid and are derived from the wild species *Musa acuminata* (A) and *Musa balbisiana* (B).^{9,10} No edible triploids of *Musa balbisiana* are known.¹¹ Sweetness and starch content also are used to classify bananas into dessert bananas, plantains, plantain cooking bananas, and “beer bananas”.¹²

Dessert bananas are preferentially consumed uncooked (i.e., raw). Meanwhile, plantain and cooking bananas are consumed at different stages of maturity. The main difference between plantain and dessert bananas is their total or partial starch-to-soluble-sugar conversion during ripening. In their ripe stage, plantains still have a high starch content (from 10% to 15% FW), which affects the taste of the banana. Therefore, plantains are preferentially consumed after processing (roasting, baking, or frying).^{12,13}

Dessert bananas convert almost all of their starch into soluble sugar during ripening.^{13,1} The difference in starch degradation

efficiency may be due to (1) the starch content of the plantains, (2) the more efficient starch degradation enzymatic apparatus in dessert bananas, and/or (3) the structural differences in the granules, which make the bananas more or less susceptible to the enzymes involved in degradation.

In addition, the susceptibility of bananas to starch degradation also depends on structural features, such as the degree of crystallinity, the amylopectin branch chain length distribution, the amylose content, and the shape and size of the granules.^{14–16}

Starch granules consist of two structurally different α -D-glucose polysaccharides: amylose and amylopectin. Amylose is essentially linear $\alpha(1-4)$ -glucan, and up to 5% of the glucose units are connected through $\alpha(1-6)$ branches in amylopectin. Starch organizes in alternating semicrystalline and amorphous layers, also known as growth rings.¹⁷ The semicrystalline layers are composed of amorphous and crystalline lamellae with a repetition period of about 9 nm.^{18–21} The crystalline lamellae are associated with the helical arrangement of amylopectin, and different patterns of crystallinity are observed depending on the organization of the helices.^{22,15}

On the basis of their X-ray diffraction patterns, starch granules are classified into two allomorphic categories: A-type (mainly cereal, tapioca, and mango starches) and B-type (potato and some tropical tuber starches).^{23–26} A third class of starch, C-type, is a mixture of A- and B-type allomorphs and can be found in some legumes and bananas (cv. Nanicão).^{21,27,28}

Received: August 26, 2010

Accepted: May 18, 2011

Revised: May 17, 2011

Published: May 18, 2011

To elucidate how starch granule structure influences degradation in banana fruits, we evaluated some structural aspects of different banana cultivars that differ in their starch accumulation and degradation and in the activities of the main enzymes involved in starch degradation.

In this work, four bananas cultivars (two dessert, Pacovan [AAB] and Mysore [AAB], and two plantains, Terra [AAB] and Figo [ABB]) at two ripening stages (green and ripe) were chosen on the basis of the differences in their starch accumulation and degradation profiles. Scanning electron microscopy (SEM) and optical microscopy (OM) were used to investigate the shapes, sizes, degradation profiles, and crystallinities of the granules during ripening. The structural details of the granules, such as the degree of crystallinity and the amylopectin branch chain length distribution, were determined by wide-angle X-ray diffraction (WAXD) and high-performance anion-exchange chromatography equipped with a pulsed amperometric detector (HPAEC-PAD), respectively. The activities of α - and β -amylases were estimated in the soluble fraction of the banana pulp and in the fraction associated with the granule starch. Starch-phosphorylase activities were only estimated in the soluble fraction of the pulp. The influence of enzyme on starch granule structure under starch degradation process was performed by digestion *in vitro* with α -amylase.

MATERIALS AND METHODS

Materials. Banana fruit (*Musa acuminata* L.) from the Mysore (AAB) dessert banana and the Terra (AAB) and Figo (ABB) plantains were harvested in Itapetinga (São Paulo State, Brazil). The Pacovan (AAB) dessert bananas were donated by the Centro de Pesquisa Apta Regional, which is located in Registro (São Paulo State, Brazil). The dessert bananas and plantains were stored at 20 °C and 90% moisture for approximately 110 days after anthesis (DAA). The samples were selected on the basis of their respiration and ethylene production during the pre- and postclimacteric stages, including the first stage of senescence. Each sample was composed of at least 10 banana fingers, which were peeled, sliced, frozen in liquid N₂, and then stored at -80 °C.

Ethylene and CO₂ Production. For the ethylene and CO₂ measurements, the fruits were enclosed in jars for 1 h, and the headspace gas was analyzed by gas chromatography as previously described by Purgatto et al.²⁹ An HP-Plot Q (30 Mts., i.d. 0.53 mm, Agilent Technologies) column was used for both gases; the injector and detector temperatures were both 250 °C, and the runs were isothermic at 30 °C. The fluxes of the helium carrier gas were 1 mL/min for ethylene and 4 mL/min for CO₂. The injections were performed in pulsed splitless mode for the ethylene and CO₂ analyses (50:1). Ethylene and CO₂ standards (Air-Liquide LTD) were used for the calibration curves.

Starch Content. Approximately 0.5 g of dessert banana and plantain pulps were homogenized in 5 mL of 0.5 M NaOH and then neutralized with 5 mL of 0.5 M acetic acid. Afterward, the volume was raised to 25 mL with distilled water. A 1 mL aliquot was washed twice with 4 mL of 80% ethanol. The total starch in the residue was quantified: (1) enzymatically, using amyloglucosidase to first hydrolyze the starch followed by quantifying the free glucose using a glucose-oxidase/peroxidase/ABTS system, as previously described by Cordenunsi and Lajolo,¹ and (2) chemically, using 10 mL of 0.25 M H₂SO₄ to hydrolyze the starch followed by quantifying the free glucose, as outlined by Trevelyan and Harrison.³⁰

Amylose Content. The total amylose content of the starch granules was determined enzymatically using a Megazyme kit (amylose/amylopectin) from Megazyme International Ltd., Bray Business Park, Bray, Wicklow, Ireland.

Isolation of Starch Granules. Starch granules were isolated from the fruit pulp at two different ripening stages, as previously described by Simão et al.²⁶ About 100 g of banana pulp was homogenized in 300 mL of 100 mM HEPES-KOH, pH 8.0, containing 1 mM EDTA, 5 mM DTT, and 0.05% Triton X-100. The homogenate was filtered through a Miracloth membrane (Calbiochem), and the filtrate was decanted overnight at 4 °C. The major supernatant was discarded, and the aqueous pellet was subjected to a 95% Percoll gradient (GE healthcare, Amersham Biosciences). After 30 min at -4 °C, the solution was centrifuged, the pellet was washed with 500 mM HEPES-KOH, pH 7.0, dried under a vacuum (spped-vac), and stored at -20 °C. In the first stage, the starch was extracted from the green bananas immediately after harvest. In the second stage, the granules were obtained from the banana fruits during full ripening.

Branch Chain Length Distribution Analysis. Amylopectin was debranched with *Pseudomonas* isoamylase according to the method described by Jane et al.³¹ On the basis of the publications of Koch et al.³² and Jacobs et al.,³³ the amylopectin branch chain length distribution was determined using a high-performance anion-exchange chromatograph equipped with a pulsed amperometric detector (HPAEC-PAD).

Wide-Angle X-ray Diffraction (WAXD). The WAXD diagrams were recorded using a rotating-anode X-ray diffractometer (Rigaku Corporation, Danvers, MA, USA) with Ni-filtered CuK α radiation ($\lambda = 1.542 \text{ \AA}$) operating at 50 kV and 100 mA at the Brazilian Synchrotron Light Laboratory (Campinas, Brazil). A Mar345 image plate placed 200.0 mm away from the sample recorded the diffraction patterns for 10 min. An alumina pattern was used for calibration. Prior to the measurements, the water contents of the samples were adjusted by sorption at 90% relative humidity for 10 days in the presence of a saturated sodium chloride solution under a partial vacuum. The samples were prepared in glass capillary tubes with diameters of 0.7 mm. The capillary tubes were centrifuged to pack the granules at the bottom and sealed to prevent any significant changes in their water content during the measurement. The WAXD profiles were obtained by radial averaging and integrated between $2\theta = 5$ and 40° . The relative crystallinity and proportions of the A- and B-type allomorphs were also determined.³⁴

Scanning Electron Microscopy (SEM). The dried starch was fixed onto stubs with double-sided tape and coated with a 10-nm-thick platinum layer using the Bal-Tec MED-020 coating system. The samples were examined on a Quanta-600 scanning electron microscope (FEI, Eindhoven, Netherlands). SEM was performed in secondary electron mode at 2–5 kV.

Protein Extraction and α - and β -Amylase Activities in the Pulp. The activities of α - and β -amylases in the pulp were determined according to the method of Peroni et al.³⁵ Frozen pulp (0.5 g) was extracted in 2 mL of 50 mM HEPES-KOH (pH 7.0) containing 20 mM cysteine, 100 mM benzimidazole, and 1% polyvinylpyrrolidone 40 (PVP-40). The supernatant (after centrifugation at 12,000g for 15 min) was considered to be the crude extract. The *in vitro* activities were measured after incubating the crude extract (20 μ L) with 20 μ L of specific substrates for α -amylase (BPNPG7, Ceralpha) or β -amylase (BPNPG5, Betamyl), both from Megazyme International Ltd., Bray Business Park, Bray, Wicklow, Ireland. The protein levels were quantified according to the Bradford³⁶ method. The activities were expressed as μ mol of *p*-nitrophenyl (PNP) released per hour.

Protein Extraction and α - and β -Amylase Activities in the Starch Granules. Protein extraction was performed according to the method described by Peroni et al.³⁵ The same assay conditions used for the soluble enzymes in the pulp were adopted for the α - and β -amylase activities in the starch granules. The activities were expressed as μ mol of *p*-nitrophenyl (PNP) released per hour.

Native PAGE Gels for Starch-Phosphorylase Activity. The crude extract containing the protein was obtained according to Mainardi

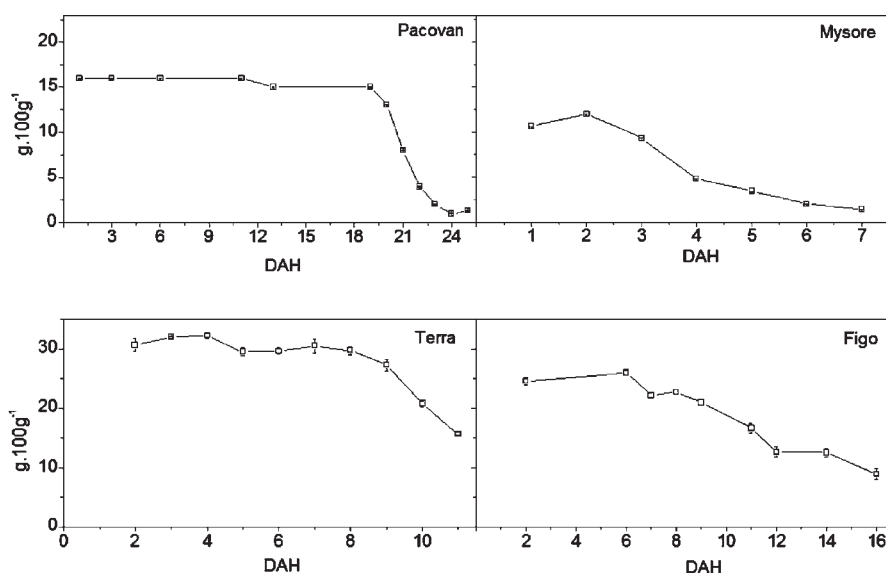


Figure 1. Starch degradation profiles of the banana cultivars. The symbols represent the means ($n = 3$), and the bars represent the standard deviations. DAH: days after harvest.

et al.⁷ Half a gram of frozen pulp was extracted in 2 mL of 50 mM HEPES-KOH (pH 7.0) containing 20 mM cysteine, 100 mM benzamidine, and 1% polyvinylpyrrolidone 40 (PVP-40). The supernatant (after centrifugation at 12,000g for 15 min) was considered to be the crude extract. The assay was performed using a native polyacrylamide gel (7.5%) containing glycogen (25 $\mu\text{g}/\text{mL}$ per gel), as described by Mota et al.³⁷

In Vitro Degradation of Native Starch Granules. Twenty milligrams of starch granules isolated from green stage of banana cultivars were prepared for in vitro degradation according to the methodology described by Reimann et al.³⁸ The starch granules were deproteinated using water/toluene (3:1) solution. The 1.2 mL water/toluene solution was vigorously mixed (30 s) with the starch granules and then separated by centrifugation (16,000g, 5 min). This operation was repeated four times followed by three washes with 1 mL of water to guarantee that the water/toluene solution was removed. Then, the starch granules were incubated under rotation using 50 mM HEPES-KOH (pH 7.0) containing 20 mM cysteine and 100 mM benzamidine added to α -amylase (3 $\text{U} \cdot \text{mg}^{-1}$ of starch), thermostable, from Megazyme International Ltd., Bray Business Park, Bray, Wicklow, Ireland, for 12, 24, 48, and 72 h at 37 °C. The enzyme had 3,000 $\text{U} \cdot \text{mL}^{-1}$ of activity based on the Ceralpha method. The control of analyses was conducted by incubation of starch granules only with 50 mM HEPES-KOH (pH 7.0) containing 20 mM cysteine and 100 mM benzamidine.

RESULTS AND DISCUSSION

Starch Degradation during the Ripening of Dessert Bananas and Plantains. During the experiments, we realized that the starches from the plantains (Terra and Figo) were not fully hydrolyzed into glucose by amyloglucosidase treatment, underestimating the total starch content of the plantains by about 50%. For the dessert bananas, the starch contents obtained using the two methodologies were similar (about 16% for Pacovan and 12% for Mysore). This result was the first suggestion that plantain starches resist the actions of enzymes that are linked to starch metabolism.

The cultivars differed in their total starch accumulation during development, as can be seen in the green fruit (Terra, 30%; Figo,

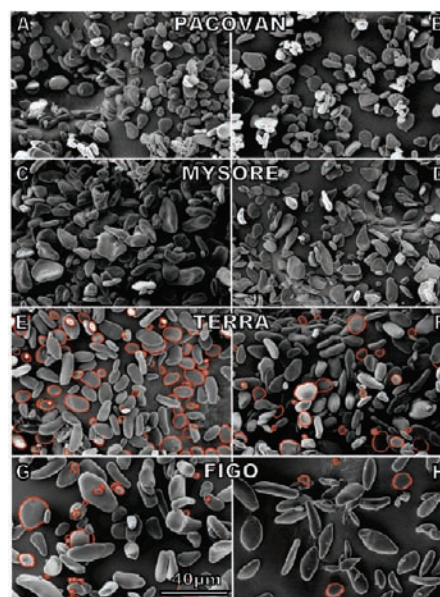


Figure 2. SEM images of the banana cultivars at the green (A, C, E, and G) and ripe (B, D, F, and H) stages. The red lines show the small and round granules, which are preferentially degraded during plantain ripening.

25%; Pacovan, 16%; and Mysore, 12%; Figure 1), in the residual starch after ripening (Terra, 16%; Figo, 9%; Pacovan, 1%; and Mysore, 1%), and at the onset of starch degradation. The differences in the times to start and complete starch degradation were not related to the physiological maturities of the fruits. Namely, the respiration and ethylene profiles indicated that all of the cultivars were in the preclimacteric stage when the experiments began (Supporting Information).

Starch Granule Surface Characterization of Bananas and Plantains during Ripening. Figure 2 shows SEM micrographs of the starch granules isolated from green and ripe banana fruits.

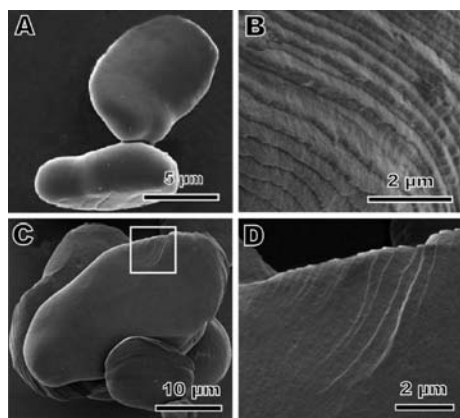


Figure 3. High-magnification SEM image of (A) starch granules isolated from the Pacovan dessert banana at the green stage. High-magnification SEM image of (B) starch showing exposition during ripening. SEM image of (C) starch granules from the region near the apexes of the granules. High-magnification SEM image of (D) the demarcated area in C.

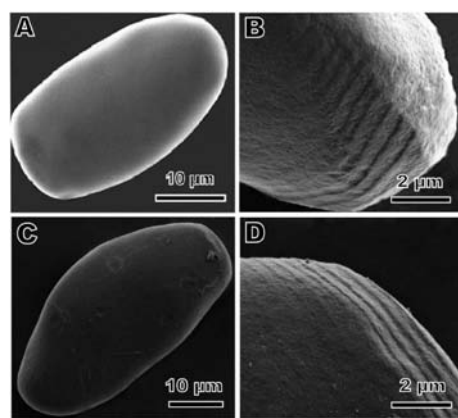


Figure 5. High-magnification SEM image of (A) starch granules isolated from the Terra plantain at the green stage. High-magnification SEM image of (B) starch granules extracted at the ripe stage, showing the exposition next to the apexes of the starch granules. High-magnification SEM image (C) showing the starch degradation profile. High-magnification SEM image of (D) the starch presented in C.

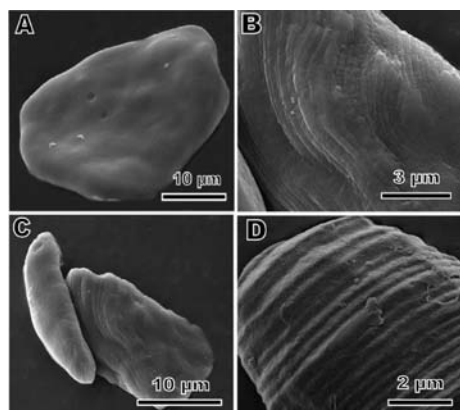


Figure 4. (A) High-magnification SEM image of starch granules isolated from the Mysore dessert banana at the green stage. High-magnification SEM images (B–D) of starch showing exposition during ripening.

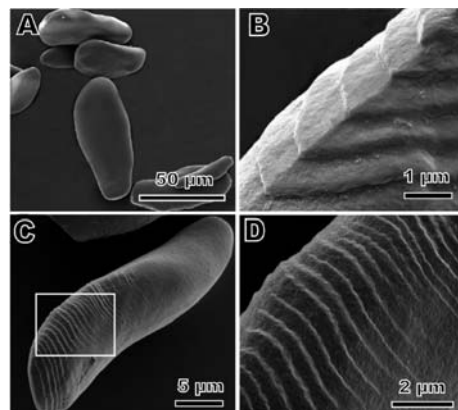


Figure 6. (A) High-magnification SEM image of starch granules isolated from the Figo plantain at the green stage. High-magnification SEM images of (B) starch granules extracted from the ripe stage, showing exposition. High-magnification SEM image (C) at a pronounced stage of degradation. High-magnification SEM image (D) of the area shown in C.

The starch granules of the green dessert bananas (Pacovan and Mysore) were small and mainly leaf-like. By contrast, the plantains (Terra and Figo) were predominantly round and elongated. Starch granules with elongated shapes were observed in all of the cultivars at the ripe fruit stage as a result of degradation. For the plantains, the small and round granules almost disappeared in the ripe stage (Figure 2E to H; granules circled by red lines), which may be due to the greater susceptibility of the small round granules to enzymatic degradation. Kong et al.³⁹ and Salman et al.¹⁶ found similar results for cereal starches.

In addition, the larger round and elongated granules with smooth surfaces exhibited few signs of degradation. The leaf-like shapes of the granule starches in the dessert bananas increased the susceptibility of the starches to enzymatic attack relative to the rounded granules of the plantains, probably because of the amylopectin arrangement.⁴⁰

The high-magnification SEM images revealed starch granule surface details during ripening (Figures 3 to 6) in all of the banana cultivars. The Pacovan dessert banana exhibited seemingly

smooth surfaces with no signs of degradation (Figure 3A). At the ripe stage, some details of the granule surface could be found. The micrographs revealed that starch degradation occurred layer by layer (Figure 3B) and stopped near the apexes of the granules (Figures 3C to D). The layers were observed at regular distance intervals (~ 150 – 300 nm), as shown in Figure 3B.

SEM images of the starch granules extracted from Mysore revealed some pits on the granule surface in the green stage, indicating that ripening starts earliest in this cultivar (Figure 4A). Layer exposition was observed in Mysore bananas, occurring differently, with some starch granules exhibiting an exposed layer (Figure 4B to C) and others located around the apexes (Figure 4D) with a regular distance interval of 300 nm between adjacent layers.

The plantains (Terra and Figo), like the Pacovan, exhibited smooth and regular surfaces in the green stage, with no signs of degradation (Figures 5A and 6A). Signs of corrosion on the Terra starch granule surfaces were very subtle and only appeared

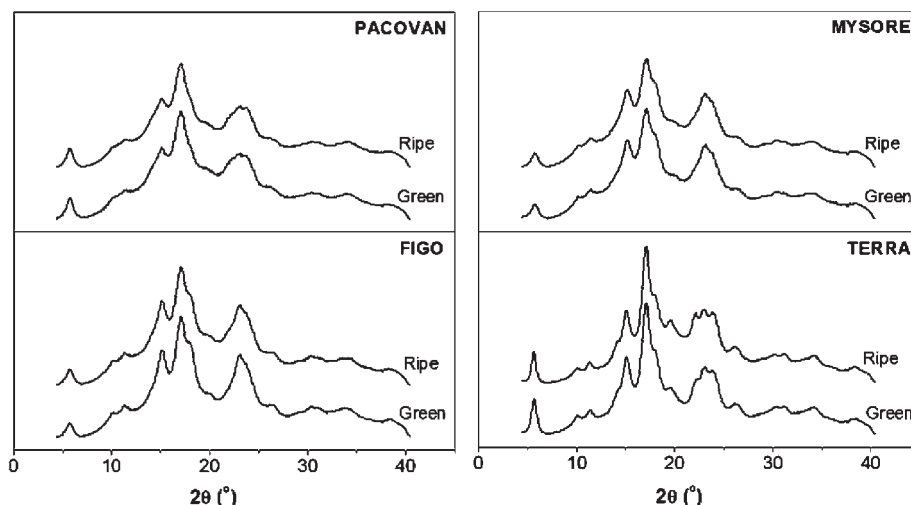


Figure 7. WAXD patterns of the starches extracted from dessert and plantain bananas at the green and ripe stages.

around the starch granule apices during the ripe stage (Figure 5B–D). In the Figo plantain, signs of starch degradation were also more evident next to the granule apices (Figure 6B,C). The distance between the layers in the plantains ranged from 150 to 500 nm (Figures 5D and 6B). In the Figo plantain, layer exposition seemed to be deeper and larger compared to other cultivars (Figure 6D).

The layers near the apices of the starch granules can be attributed to the vestiges of starch degradation. Once a layer becomes more elevated in the starch granule apices, it suggests that this region is naturally more resistant to degradation. The regular exposition can be related to the radial alignment of the crystalline structures within the starch granule, as observed in the starch granules of peas⁴¹ and confirmed in the starch granules of bananas (cv. Nanicão) using AFM.²⁸ The radial alignment of the crystalline structures in these starches was confirmed by the presence of the Maltese crosses that persisted until the ripe stage, indicating that starch degradation did not affect this alignment (Supporting Information).

Structural Characterization of Starch Granules. *Crystallinity Index (CI).* The wide-angle X-ray diffraction (WAXD) patterns for all of the banana cultivars are presented in Figure 7. All of the spectra had a C-type allomorph profile, indicating the coexistence of A- and B-type crystallites in the samples. The differences between the WAXD diagrams are related to the different degrees of crystallinity and the relative abundances of each allomorph in the samples (Table 1). Terra and Pacovan (green and ripe starch granules) were mainly dominated by a B-type allomorph pattern based on peaks at $2\theta = 5.6, 17.0, 22.0,$ and 24.0° . By contrast, the Figo and Mysore cultivars had diffraction patterns characterized by the specific reflections of an A-type allomorph ($2\theta = 18.0, 20.0,$ and 23.0°). No significant changes in the A/B-type allomorph ratio were observed for the Terra, Pacovan, and Mysore cultivars during ripening. However, a significant degradation of A-type crystallites was observed in the Figo cultivar during starch degradation.

Similarities and differences in the crystallinity index were observed when the banana starches were compared (Table 1). Pacovan and Mysore had crystallinities around 20%, while the crystallinities of the Figo and Terra cultivars were $\sim 24\%$ and 30% , respectively. With the exception of Terra, the crystallinity index does not seem to depend on ripening because practically

no changes in the crystallinity of the granules were observed during the stages of degradation. We consider that these differences can be related to the ability of enzyme penetration inside the granule. Then, we speculate that this penetration is dependent on the presence of pores as well as the lamellar organization of starch.

Amylopectin. The branch chain length distribution of amylopectin had a bimodal distribution for all of the cultivars at the green and ripe stages. A distinct peak was observed at a degree of polymerization (DP) of 12–14, and a second population was observed next to DP 40 (Supporting Information). According to Hanashiro et al.,⁴¹ the amylopectin chain length can be classified into external short chains *fa* (DP 6–12), *fb*₁ (DP 13–24), and *fb*₂ (DP 25–36), and long chains *fb*₃ (DP > 37).

The results summarized in Table 1 indicate that all of the cultivars had a larger proportion of the short *fa*-chain (24.2% for Mysore to 28.8% for Pacovan) and *fb*₁-chain (50.7% for Figo and 56.3% for Mysore) amylopectin. These results were nearly identical during both ripening stages. The number of long amylopectin *fb*₃-chains (DP ≥ 37) decreased from the green to the ripe stage for most of the cultivars (with the exception of Pacovan), varying from 6.0% (Mysore) to 7.3% (Pacovan).

In this work, we used the following ratio to estimate the amylopectin chain length:⁴²

$$fa/fb_{1-3} = \frac{fa}{fb_1 + fb_2 + fb_3} \quad (1)$$

Larger ratios reveal the degree of amylopectin ramification. A larger proportion of short chains correspond to a higher crystallinity index for the starch granule. The *fa/fb*_{1–3} values obtained for Pacovan, Mysore, and Figo (Table 1) indicated a slight decrease in the number of short amylopectin chains during starch degradation (0.41–0.39, 0.37–0.34, and 0.34–0.32, respectively). However, Terra (Table 1) exhibited a subtle increase in the number of these chains in the mature stage (0.36–0.39). According to Jane et al.,¹⁴ the degree of crystallinity frequently depends on the proportion of amylopectin chains. The size of the *fa* (DP 6–12) fraction of the amylopectin chain length distribution plays an important role in determining the

Table 1. Starch Characteristics and Amylopectin Chain Length Distribution of Dessert and Plantain Bananas at the Green and Ripe Stages

starch characteristics (%)	dessert bananas				plantain			
	Pacovan		Mysore		Terra		Figo	
	green	ripe	green	ripe	green	ripe	green	ripe
starch ^a	61.0 ± 2.6	4.3 ± 0.6	44.4 ± 2.8	5.7 ± 0.4	76.4 ± 2.8	41.1 ± 0.7	73.9 ± 1.8	28.4 ± 3.0
amylose	18.9 ± 1.2	20.7 ± 0.8	15.2 ± 0.7	14.8 ± 0.6	21.2 ± 3.1	21.7 ± 0.9	24.1 ± 1.0	18.5 ± 0.3
CI ^b	19.0	19.3	21.8	21.5	30.5	26.2	24.7	23.8
A/B ratio	0.54	0.52	1.44	1.44	0.67	0.61	2.03	1.27
Amylopectin Chain Length Distribution (%)								
<i>fa</i> ^c	28.8	28.3	25.4	24.2	26.9	28.3	27.0	25.4
<i>fb</i> ₁	52.1	51.5	52.8	56.3	55.3	52.1	50.7	54.2
<i>fb</i> ₂	12.3	12.9	15.1	13.6	14.0	13.4	13.4	14.2
<i>fb</i> ₃	6.7	7.3	6.7	6.0	6.3	6.2	6.2	6.1
<i>fa/fb</i> _(1–3)	0.41	0.39	0.34	0.32	0.36	0.39	0.39	0.34

^a Starch content was expressed in dry matter (DM). ^b CI: crystallinity index; the values represent the mean of 3 (starch) and 2 (amylose) replicates ± the standard deviation. ^c Amylopectin chain length was classified as follows: *fa*, DP 6–12; *fb*₁, DP 13–24; *fb*₂, DP 25–36; and *fb*₃, DP ≥ 37.

polymorphic forms of starch crystals, which could contribute to the slower rate of starch degradation in the Terra plantain.

In our results, this relationship was not observed (except for the Terra plantain) because the short amylopectin chain lengths were similar across the cultivars, even though the degrees of crystallinity were different (Table 1). We observed that the degree of crystallinity was reduced concomitantly with the proportion of amylopectin short chains (*fa* and *fb*₁-chains) for the Pacovan, Mysore, and Figo cultivars, indicating that the corrosion of the granules does not affect the crystallinity profile or the degree of crystallinity of the granules. In the Terra cultivar, a subtle increase in the *fa/fb*_{1–3} ratio could explain the higher degree of crystallinity and the lower degradation rate of its granule.

Amylose. The amylose content was greater in plantain cultivars (21 to 24%) than in dessert banana cultivars (15 to 19%) (Table 1). The amylose contents of the dessert bananas and Terra were almost constant during degradation. However, the amylose content of Figo decreased by about 23% during degradation. This decrease can be interpreted as (1) a result of starch degradation by the exocorrosion of the amylose-rich layers, which was also found in maize starch,⁴³ or (2) the existence of two granule populations in this cultivar, one of which is more susceptible to degradation (Figure 2G–H). Two facts support the second hypothesis. First, the small and round granules in the starch of the mature green Figo cultivar almost disappear from the population of granules isolated from the ripe Figo cultivar (Figure 2H). Furthermore, the A/B-type allomorph ratio (2.03 to 1.27) was drastically reduced between the stages. Small and round granules have been reported to be more susceptible to degradation.^{39,16} Moreover, the A/B-type allomorph ratio reduction suggests that round starch granules are predominantly A-type.

Pacovan and Terra had similar initial amylose contents, but the starch degradation rates were different. These differences indicate that other characteristics, such as the distribution of the amylose matrix and granule size and shape (Table 1), can also be involved in degradation. We found a stronger correlation between amylose content and the crystallinity index than with the distribution of the branch chain length of amylopectin.

α- and β-Amylase Activities in the Pulp and Associated with the Starch Granule of Bananas. *Soluble Enzymes.* The activities of soluble α- and β-amylase were detected in the pulp of all cultivars starting at the initial ripening stage (Figure 8). The dessert bananas had maximum α-amylase activities of under 2 μmol PNP/h, while plantains had maximum activities between 2 and 6 μmol PNP/h. The soluble β-amylase activity increased throughout ripening and reached its maximum value in the later stages of ripening in all of the cultivars (Figure 8). Figo had similar amounts of α- and β-amylase activities in the ripe stage (14 DAH). At the same time, the β-amylase activity was 3 to 6 times higher than the α-amylase activity for Terra, Mysore, and Pacovan in the mature stage (Figure 8).

The α-amylase activities were almost constant during banana ripening in all cultivars, except for Figo, which showed the highest content of amylose (24%) and granule size.

Native PAGE revealed two protein bands with activities that can be associated with cytosolic (PHO 1) and plastidial (PHO 2) starch-phosphorylases isoforms (Figure 8). The two isoforms showed some activity during all of the ripening stages in all of the cultivars (except for Mysore). The highest activities were observed in the plantains (Terra and Figo), with PHO 1 higher than PHO 2. Although the Pacovan starch-phosphorylases exhibited less intense activity bands, they were constant during fruit ripening (Figure 8).

The presence of soluble α- and β-amylase activities (Figure 9), concomitant with the absence and/or low intensity of the starch-phosphorylase bands, indicates that hydrolytic degradation is the major route of degradation in banana starch. This was already seen in the Nanição cultivar and in the mango.^{37,28}

Enzymes Associated with Starch Granules. The initial values of the α- and β-amylase activities associated with starch granules (Figure 9) were several times higher than the activities in the pulp (Figure 8) and remained constant throughout degradation. Similar to the profile observed in the pulp, the β-amylase activity was higher than the α-amylase activity, except in Mysore, which exhibited higher α-amylase activity in the earlier stages of ripening. Remember that Mysore (Figure 4) was the one cultivar whose starch showed signs of degradation (pits) starting at the

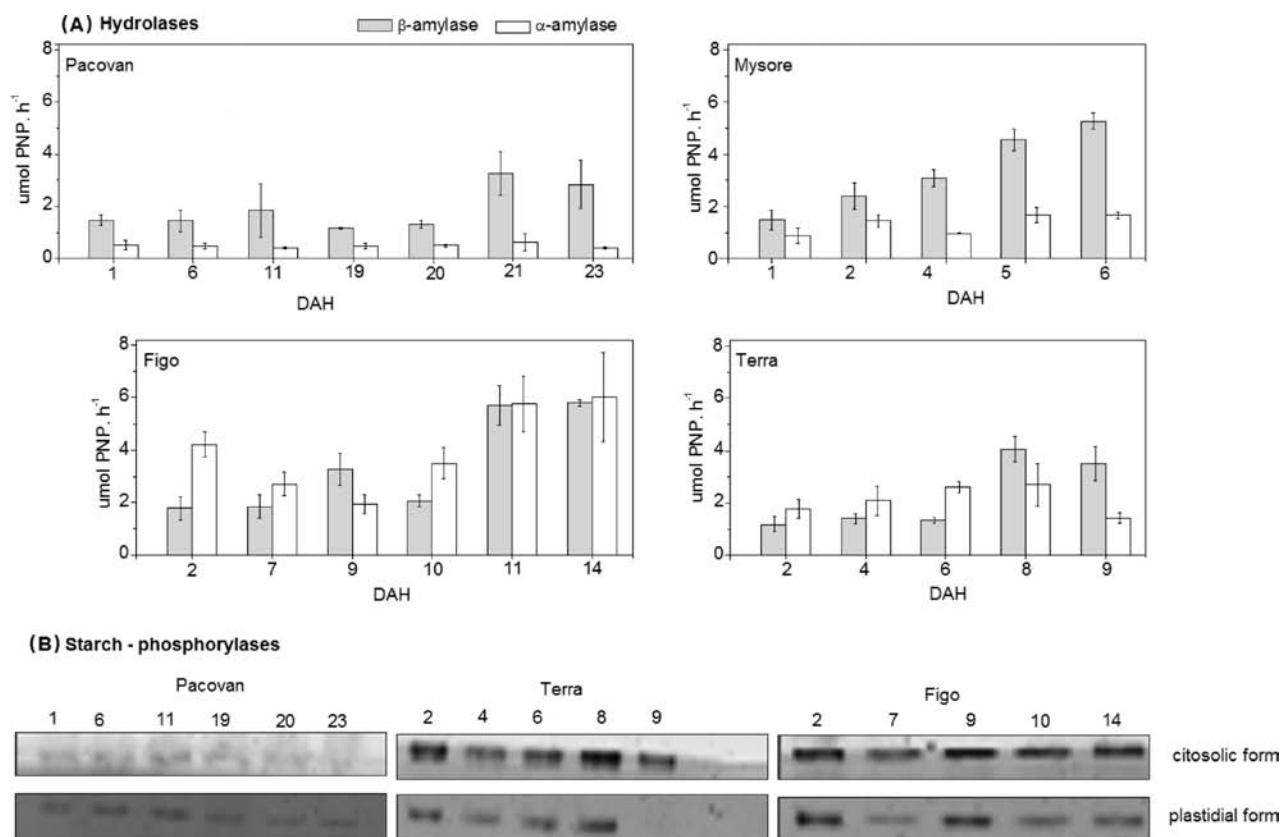


Figure 8. (A) Activities of α -amylase (white column) and β -amylase (gray column) in the pulp of the banana cultivars at different points during ripening. (B) Native PAGE (7.5%) with glycogen (25 μ g/mL) to detect the starch-phosphorylases soluble in the pulps of the banana cultivars at different days during ripening. After electrophoresis (at 4 $^{\circ}$ C and 15 mA/gel), the gel was washed twice with 100 mM citrate/NaOH (pH 6) and incubated for 2 h at 37 $^{\circ}$ C in the same buffer added with 0.005% of soluble starch and 20 mM of glucose-1-phosphate. The bands were revealed by staining the gel with Lugol's solution (13 mM I_2 and 40 mM KI).

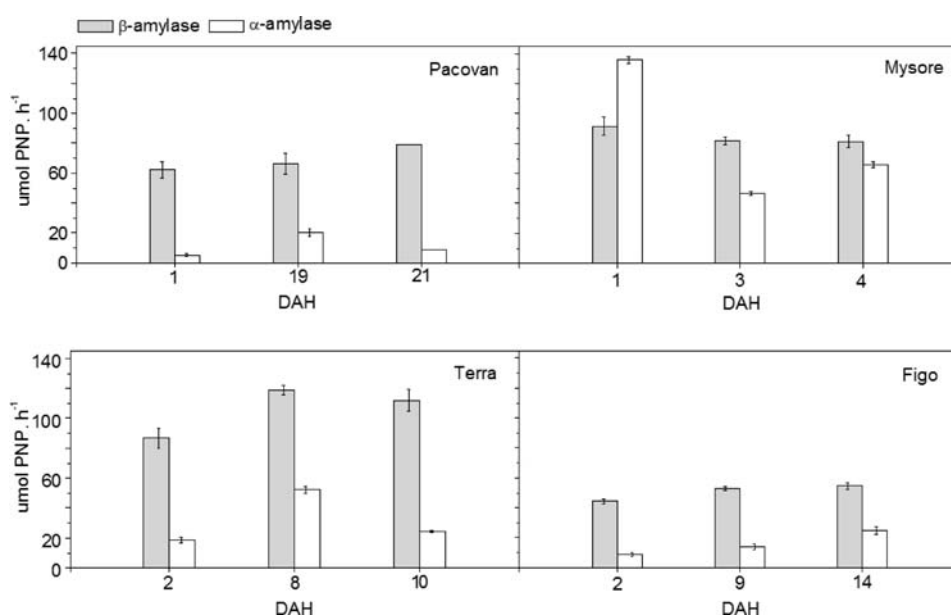


Figure 9. Activities of α -amylase (white column) and β -amylase (gray column) associated with the starch granules extracted from the banana cultivars at different points during ripening. The columns represent the means ($n = 3$), and the bars represent the standard deviations.

first stage after harvest. At the same time, we were unable to detect any starch phosphorylase activity in Mysore (Figure 8),

and starch phosphorylase activity was barely detected in Pacovan. In the plantains, starch phosphorylases were detected during all

ripening stages. Given the maximum activities of the hydrolytic enzymes associated with the granules vs the onset of starch degradation, it is possible to assume that α -amylase is the key enzyme in banana starch degradation. Starch phosphorylases were not detected in the granules but were already seen for cv. Nanicão.²⁸

It is important to note that both α - and β -amylases are already associated with the starch granule, even when there are no signs of degradation in the granule, as seen in the results. The quantity of starch remains the same for several days in some cultivars, such as Pacovan and Terra, on the basis of the images of the granule surfaces with no signs of corrosion and the presence of soluble sugars derived from starch degradation.

Reimann et al.⁴⁴ observed that the association of α -amylase with the starch granule of *turions* precedes starch degradation. However, the question remains: what triggers degradation if the enzymes that are supposedly linked to degradation are already associated with the granules days before the start of degradation?

Degradation appears to start at initial pits on the surfaces of the granules, and these pits became associated with α -amylase activity once Mysore showed a pronounced presence of pits on the starch granule surface concomitant with strong α -amylase activity (Figures 4A and 9, respectively).

We can associate the differences in starch degradation with amylose distribution inside the granule. As already verified in pea starches, the size of crystalline lamella is increased concomitantly with the increase of amylose content.¹⁷ Then, assuming that the same pattern can occur in the banana cultivars, the enlargement of the crystalline lamella causes the starch granules of the plantains to become more resistant to enzymatic degradation. This explains the high levels of α - and β -amylase activity that are associated with the starch granule (Figure 9) and observed in all of the cultivars. It also explains the slow degradation rate of the plantains.

In Vitro Native Starch Granule Degradation. The influence of starch granule structure under the starch degradation process was investigated using in vitro degradation of starch granules with α -amylase during 72 h (samples were taken at 24, 36, and 72 h). The α -amylase action caused different changes in the starch granules according to the cultivar (Figure 10). As happened by natural starch degradation (actions of enzymes naturally present in the banana), the granules isolated from dessert bananas (Mysore and Pacovan) showed stronger signs of degradation (Figure 10A, B) than plantains (Terra and Figo, Figure 10C,D).

After 24 h, the surface of Terra starch granules were practically the same as that of the control (Supporting Information), but we found few granules with the interior entirely corroded preserving the shells that cover the surface of the granules. It seems that the enzyme found a weak spot at the top of the granule and became degraded (Figure 10 C). In a previous work,²⁸ the data obtained by atomic force microscopy supported the idea that the first layer covering the starch granules of banana (cv. Nanicão, a dessert banana) is composed of a hard or well organized material that once removed easily turns on the action of the enzymes of starch degradation. Maybe Terra starch is an extreme example of this theory, which relies on very special conditions to degrade these first layers, which were not obtained in in vitro conditions. It is necessary to emphasize that we never find this kind of corrosion in the granules isolated from ripened Terra, in natural conditions. In Figo starches, this kind of degradation was not found. As matter of fact, after 24 h in contact with α -amylase only very few signs of corrosion were observed. At the same time, the granules of Mysore and Pacovan showed signs of extensive degradation. These results support previous findings that the structure of

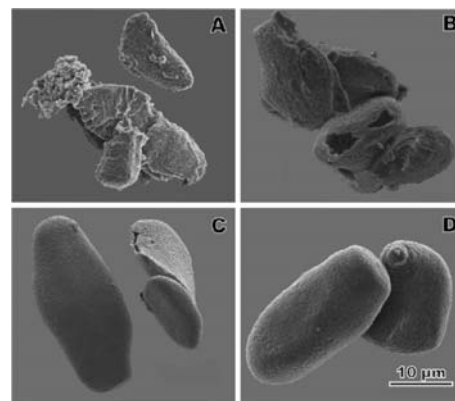


Figure 10. In vitro degradation of native starch granules isolated from green banana pulp of (A) Mysore, (B) Pacovan, (C) Terra, and (D) Figo, visualized by high-magnification SEM. Starches were incubated with buffer (50 mM HEPES-KOH (pH 7.0) containing 20 mM cysteine and 100 mM benzamidine) added to α -amylase ($3 \text{ U} \cdot \text{mg}^{-1}$ of starch) during 24 h at 37°C .

plantains starches is more resistant to degradation caused by endogenous enzymes.

Here, we provide evidence that it is important to consider starch granule structure when discussing differences in starch degradation of dessert bananas vs plantains. Plantains accumulate the largest amounts of starch, strong enzyme activities, and amylose (Figo), and exhibit a higher degree of crystallinity (Terra) than dessert bananas. Plantains had mainly long and round starch granules, while leaf-like shapes were predominant in the dessert bananas. The crystallinity profiles and sizes of the amylopectin chains do not seem to affect the susceptibility of the granules to degradation.

■ ASSOCIATED CONTENT

S Supporting Information. Ethylene and CO_2 production of banana cultivars, optical and polarizing images of banana starches, amylopectin chain length distribution of banana starches, and control of the Figure 10 high-magnification SEM image of banana starches. This material is available free of charge via the Internet at <http://pubs.acs.org>.

■ AUTHOR INFORMATION

Corresponding Author

*Phone: +55-11-30913656. Fax: +55-11-38154410. E-mail: hojak@usp.br

Funding Sources

This work was supported by CNPq and FAPESP. LNLS was supported by project MX1-6948 (XRD).

■ ACKNOWLEDGMENT

We acknowledge the Centro de Pesquisa Apta Regional, located in Registro (São Paulo State, Brazil), for material donations.

■ ABBREVIATIONS USED

SEM, scanning electron microscopy; DAA, days after anthesis; NaOH, sodium hydroxide; HEPES, 4-(hydroxyethyl)-1-piperazineethanesulfonic acid; KOH, potassium hydroxide; EDTA,

ethylenediamine tetraacetic acid; DTT, 1,4-dithiothreitol; HPAEC-PAD, high performance anion exchange chromatography with pulse amperometric detection; WAXD, wide-angle X-ray diffraction; PVP-40, polyvinylpyrrolidone-40; PNP, *p*-nitrophenyl; AFM, atomic force microscopy; PHO, starch-phosphorylase; DAH, days after harvest.

REFERENCES

- (1) Cordenunsi, B. R.; Lajolo, F. M. Starch breakdown during banana ripening: Sucrose synthase and sucrose phosphate synthase. *J. Agric. Food Chem.* **1995**, *43*, 347–351.
- (2) Mota, R. V.; Lajolo, F. M.; Cordenunsi, B. R. Composição em carboidratos de alguns cultivares de banana (*Musa* spp.) durante o amadurecimento. *Ciênc. Tecnol. Aliment. (Campinas, Braz.)* **1997**, *17*, 94–97.
- (3) Nascimento, J. R. O.; Vieira-Júnior, A.; Bassinello, P. Z.; Cordenunsi, B. R.; Mainardi, J. A.; Lajolo, F. M. Beta-amylase expression and degradation during banana ripening. *Postharvest Biol. Technol.* **2006**, *40*, 41–77.
- (4) Purgatto, E.; Lajolo, F. M.; Nascimento, J. R. O.; Cordenunsi, B. R. The onset of starch degradation during banana ripening is concomitant to changes in the content of free and conjugated forms of indole-3-acetic acid. *J. Plant Physiol.* **2002**, *159*, 1105–1111.
- (5) Bierhals, J. D.; Lajolo, F. M.; Cordenunsi, B. R.; Nascimento, J. R. O. Activity, cloning and expression of an isoamylase-type starch-debranching enzyme from banana fruit. *J. Agric. Food Chem.* **2004**, *52*, 7412–7418.
- (6) Garcia, E.; Lajolo, F. M. Starch transformation during banana ripening: the amylase and glucosidase behavior. *J. Food Sci.* **1988**, *53*, 1181–1186.
- (7) Mainardi, J. A.; Purgatto, E.; Vieira-Júnior, A.; Bastos, W. A.; Cordenunsi, B. R.; Nascimento, J. R. O.; Lajolo, F. M. The effects of ethylene and 1-MCP on gene expression and activity profile of starch phosphorylase during banana ripening. *J. Agric. Food Chem.* **2006**, *54*, 7294–7299.
- (8) Vieira-Júnior, A.; Nascimento, J. R. O.; Lajolo, F. M. Molecular cloning and characterization of an α -amylase occurring in the pulp of ripening bananas and its expression in *Pichia pastoris*. *J. Agric. Food Chem.* **2006**, *54*, 8222–8228.
- (9) Dufour, D.; Gibert, O.; Giraldo, A.; Sánchez, T.; Reynes, M.; Pain, J.-P.; González, A.; Fernández, A.; Díaz, A. Differentiation between cooking bananas and dessert bananas. 2. Thermal and functional characterization of cultivated Colombian Musaceae (*Musa* sp.). *J. Agric. Food Chem.* **2009**, *57*, 7870–7876.
- (10) Zhang, P.; Whistler, R. L.; Bemiller, J. N.; Hamaker, B. Banana starch: production, physicochemical properties, and digestibility: A review. *Carbohydr. Polym.* **2005**, *59*, 443–458.
- (11) Choudhury, S. R.; Roy, S.; Saha, P. P.; Singh, S. K.; Sengupta, D. N. Characterization of differential ripening pattern in association with ethylene biosynthesis in the fruits of five naturally occurring banana cultivars and detection of a GCC-box-specific DNA-binding protein. *Plant Cell Rep.* **2008**, *27*, 1235–1249.
- (12) Heslop-Harrison, J. S.; Schwarzacher, T. Domestication, Genomics and the Future for Banana. *Ann. Bot. (Oxford, U.K.)* **2007**, *100*, 1073–1084.
- (13) Gilbert, O.; Dufour, D.; Giraldo, A.; Sánchez, T.; Reynes, M.; Pain, J.-P.; González, A.; Fernández, A.; Díaz, A. Differentiation between cooking bananas and dessert bananas. I. Morphological and compositional characterization of cultivated Colombian Musaceae (*Musa* sp.) in relation to consumer preferences. *J. Agric. Food Chem.* **2009**, *57*, 7857–7869.
- (14) Jane, J.-L.; Wong, K.-S.; McPherson, A. E. Branch-structure difference in starches of A- and B-type X-ray patterns revealed by their Naegeli dextrans. *Carbohydr. Res.* **1997**, *300*, 219–227.
- (15) Jane, J.-L. Structure of starch granules. *J. Appl. Glycosci.* **2007**, *54*, 31–36.
- (16) Salman, H.; Blazek, J.; Lopez-Rubio, A.; Gilbert, E. P.; Hanley, T.; Copeland, L. Structure-function relationship in A and B granules from wheat starches of similar amylose content. *Carbohydr. Polym.* **2009**, *75*, 420–427.
- (17) Jenkins, P. J.; Donald, A. M. The influence of amylose on starch granule structure. *Int. J. Biol. Macromol.* **1995**, *17*, 315–321.
- (18) Calvert, P. Biopolymers - The structure of starch. *Nature* **1997**, *389* (6649), 338–339.
- (19) Cardoso, M. B.; Samios, D.; Silveira, N. P. Study of protein detection and ultrastructure of Brazilian rice starch during alkaline extraction. *Starch-Starke* **2006**, *58*, 345–352.
- (20) Sanderson, J. S.; Daniels, R. D.; Donald, A. M.; Blennow, A.; Engelsen, S. B. Exploratory SAXS and HPAEC-PAD studies of starches from diverse plant genotypes. *Carbohydr. Polym.* **2006**, *64*, 433–443.
- (21) Thys, R. C. S.; Westfahl, H.; Norena, C. P. Z.; Marczak, L. D. F.; Silveira, N. P.; Cardoso, M. B. Effect of the alkaline treatment on the ultrastructure of C-type starch granules. *Biomacromolecules.* **2008**, *9*, 1894–1901.
- (22) Cardoso, M. B.; Westfahl, H. On the lamellar distribution of starch. *Carbohydr. Polym.* **2010**, *81*, 21–28.
- (23) Beck, E.; Ziegler, P. Biosynthesis and degradation of starch in higher plants. *Annu. Rev. Plant Phys.* **1989**, *40*, 95–117.
- (24) Cardoso, M. B.; Putaux, J. L.; Samios, D.; Silveira, N. P. Influence of alkali concentration on the deproteinization and/or gelatinization of rice starch. *Carbohydr. Polym.* **2007**, *70*, 160–165.
- (25) Hoover, R. Composition, molecular structure, and physicochemical properties of tuber and root starches: a review. *Carbohydr. Polym.* **2001**, *45*, 253–267.
- (26) Simão, R. A.; Bernardes-Silva, A. P. F.; Peroni, F. H. G.; Nascimento, J. R. O.; Louro, R. P.; Lajolo, F. M.; Cordenunsi, B. R. Mango starch degradation. I. A microscopic view of the granule during ripening. *J. Agric. Food Chem.* **2008**, *56*, 7410–7415.
- (27) Wang, S.; Yu, J.; Yu, J. Conformation and location of amorphous and semi-crystalline regions in C-type starch granules revealed by SEM, NMR and XRD. *Food Chem.* **2008**, *110*, 39–46.
- (28) Peroni-Okita, F. H. G.; Simão, R. A.; Cardoso, M. B.; Soares, C. A.; Lajolo, F. M.; Cordenunsi, B. R. *In vivo* degradation of banana starch: structural characterization of the degradation process. *Carbohydr. Polym.* **2010**, *81*, 291–299.
- (29) Purgatto, E.; Lajolo, F. M.; Nascimento, J. R. O.; Cordenunsi, B. R. Inhibition of β -amylase activity, starch degradation and sucrose formation by indole-3-acetic acid during banana ripening. *Planta* **2001**, *212*, 823–828.
- (30) Trevelyan, W. E.; Harrison, J. S. Studies on yeast metabolism. I. Fractionation and microdetermination of cell carbohydrates. *Biochem. J.* **1952**, *50*, 298–302.
- (31) Jane, J.; Shen, L.; Chen, J.; Lim, S.; Kasemsuwan, T.; Nip, W. K. Physical and chemical studies of taro starches and flours. *Cereal Chem.* **1992**, *69*, 528–535.
- (32) Koch, K.; Andersson, R.; Åman, P. Quantitative analysis of amylopectin unit chains by means of high-performance anion-exchange chromatography with pulsed amperometric detection. *J. Chromatogr., A* **1998**, *800*, 199–206.
- (33) Jacobs, H.; Eerlingen, R. C.; Rouseau, N.; Colonna, P.; Delcour, J. A. Acid hydrolysis of native and annealed wheat, potato and pea starches - DSC melting features and chain length distributions of lintnerised starches. *Carbohydr. Res.* **1998**, *308*, 359–371.
- (34) Stribeck, N. *X-Ray Scattering of Soft Matter*; Springer Laboratory: Berlin, Germany, 2007.
- (35) Peroni, F. H. G.; Koike, C.; Louro, R. P.; Purgatto, E.; Nascimento, J. R. O.; Lajolo, F. M.; Cordenunsi, B. R. Mango starch degradation. II. The binding of α -amylase and β -amylase to the starch granule. *J. Agric. Food Chem.* **2008**, *56*, 7416–7421.
- (36) Bradford, M. M. Rapid and sensitive method for quantification of microgram quantities of protein utilizing of protein-dye binding. *Anal. Biochem.* **1976**, *72*, 248–254.
- (37) Mota, R. V.; Cordenunsi, B. R.; Nascimento, J. R. O.; Purgatto, E.; Rosseto, M. R. M.; Lajolo, F. M. Activity and expression of banana

starch phosphorylases during fruit development and ripening. *Planta* **2002**, *216*, 325–333.

(38) Reimann, R.; Hippler, M.; Machelett, B.; Appenroth, K. J. Light induces phosphorylation of glucan water dikinase, which precedes starch degradation in turions of the it duckweed *Spirodela polyrhiza*. *J. Plant Physiol.* **2004**, *135*, 121–128.

(39) Kong, B. W.; Kim, J. I.; Kim, M. J.; Kim, J. C. Porcine pancreatic α -amylase hydrolysis of native starch granules as a function of granule surface area. *Biotechnol. Prog.* **2003**, *19*, 1162–1166.

(40) Zihua, A.; Jane, J.-L. Characterization and modeling of the A- and B-granule starches of wheat, triticale, and barley. *Carbohydr. Polym.* **2006**, *67*, 46–55.

(41) Parker, M. L.; Kirby, A. R.; Morris, V. J. *In situ* imaging of pea starch in seeds. *Food Biophys.* **2008**, *3*, 66–76.

(42) Hanashiro, I.; Abe, J.-I.; Hizukuri, S. A periodic distribution of the chain length of amylopectin as revealed by high-performance anion-exchange chromatography. *Carbohydr. Res.* **1996**, *283*, 151.

(43) Pan, D. D.; Jane, J.-L. Internal structure of normal maize starch granules revealed by chemical surface gelatinization. *Biomacromolecules* **2000**, *1*, 126–132.

(44) Reimann, R.; Ritte, G.; Steup, M.; Appenroth, K.-J. Association of α -amilase and R1 protein with starch granules precedes the ignition of net starch degradation in turions of *Spirodela polyrhiza*. *Physiol. Plant* **2002**, *114*, 2–12.